# Scattering by a cylinder with variable bathymetry

**J. N. Newman**
jnn@mit.edu

(Submitted to 27th IWWWFB – Copenhagen, Denmark – 22-25 April 2012)

## 1 Introduction

At the last Workshop Porter [1] considered the possibility of surrounding a fixed cylinder with an annular bed of variable depth, such that there is no scattering in the far field. In this situation the cylinder is said to be 'cloaked'. Porter represented the bed depth $h(x, y)$ by a Fourier/Chebyshev expansion, and optimized the coefficients to minimize the scattered energy. Using the mild-slope approximation he showed that values of the energy close to zero could be achieved. However the resulting bed depths vary rapidly about the depth $h_2$ in the far field, as shown in Figure 2(a), implying some uncertainty regarding the validity of the mild-slope equation. The present work seeks to resolve this question by studying the same problem using the complete linear theory. A high degree of computational efficiency is required, since the optimization requires 100-1000 evaluations for different trial shapes of the bed.

In a fluid of constant depth the scattering characteristics of a body can be analyzed using the panel method. A boundary-integral equation for the unknown velocity potential is derived, using the Green function which satisfies the boundary conditions on the free surface and bottom and the radiation condition in the far field. The domain of the integral equation is restricted to the submerged surface $S_b$ of the body. After discretization the integral equation is reduced to a linear system of algebraic equations. This method can be extended to cases with variable bathymetry where $h(x, y) \le h_2$, by extending $S_b$ to include the bottom in the region of varying depth. Ferreira & Newman [2] used this approach to analyze wave effects on a ship above a sloping bottom. However it cannot be used if $h(x, y) > h_2$, as is the case for part of Porter's bed, since the Green function which satisfies the boundary condition on $z = -h_2$ is singular if $z < -h_2$. This restriction could be avoided by using a different Green function, e.g. corresponding to the maximum depth or infinite depth, but the computational domain would include the entire bottom extending to infinity. Here we consider a more efficient approach based on domain decomposition, with a matching boundary between the interior domain with variable bathymetry and the exterior domain with constant depth. Matching boundaries have been used for a variety of wave-body problems, especially for cases involving thin vertical barriers and bodies with vertical sides. Belibassakis [3] and Pinkster [4] have used matching with panel methods to analyze problems with other types of bathymetry.

## 2 Formulation and Results

Plane waves are incident from infinity and the body is fixed. Two domains $D_i$ $(i = 1, 2)$ are considered, with the corresponding velocity potentials $\phi^{(i)}$. The exterior domain $D_2$ extends to infinity, with constant depth $h_2$. In the interior domain $D_1$ the depth $h(x, y)$ is arbitrary, except that it must match the depth $h_2$ on the matching boundary $S_m$. The boundary surface of $D_1$ is $S_1$=$S_b$+$S_m$. $S_b$ includes both the body surface and the bed within $D_1$. The potential $\phi^{(2)}$ includes the incident wave $\phi_I$ and the scattering component $\phi_S$ which satisfies the radiation condition in the far field. The matching boundary separates the two domains, extending from the bottom $z = -h_2$ to the free surface $z = 0$. The unit normal is defined in each domain to be positive in the direction exterior to $D_i$.

Green's theorem is applied separately in each domain. Thus for field points $\mathbf{x}$ on the boundary surface $S_i$,

$$2\pi\phi^{(i)}(\mathbf{x}) + \iint_{S_i} \left( \phi^{(i)}(\boldsymbol{\xi}) \frac{\partial G^{(i)}(\boldsymbol{\xi};\mathbf{x})}{\partial n_\xi} - G^{(i)}(\boldsymbol{\xi};\mathbf{x}) \frac{\partial \phi^{(i)}(\boldsymbol{\xi})}{\partial n_\xi} \right) dS_\xi = \begin{pmatrix} 0 \\ 4\pi\phi_I \end{pmatrix} \qquad (i = 1, 2). \qquad (1)$$

Here $G^{(1)}$ is any Green function which is regular within $D_1$ (except at the source point), and satisfies the free-surface condition. For simplicity the conventional free-surface Green function for infinite depth is used. $G^{(2)}$ is the Green function for finite depth $h_2$. The term $4\pi\phi_I$ is included on the right-hand side since $\phi^{(2)}$ does not satisfy the radiation condition.

On $S_b$ the normal velocity $\phi_n^{(1)} = 0$, where the subscript $n$ denotes the normal derivative. The appropriate boundary conditions on $S_m$ are $\phi^{(1)} = \phi^{(2)}$ and $\phi_n^{(1)} = -\phi_n^{(2)}$. Using (1) and writing separate equations for the two domains gives the following three equations:

$$2\pi\phi^{(1)} + \iint_{S_b} \phi^{(1)} G_n^{(1)} dS_\xi + \iint_{S_m} \phi^{(2)} G_n^{(1)} dS_\xi + \iint_{S_m} G^{(1)} \phi_n^{(2)} dS_\xi = 0 \qquad (\mathbf{x} \text{ on } S_b), \qquad (2)$$

$$2\pi\phi^{(2)} + \iint_{S_b} \phi^{(1)} G_n^{(1)} dS_\xi + \iint_{S_m} \phi^{(2)} G_n^{(1)} dS_\xi + \iint_{S_m} G^{(1)} \phi_n^{(2)} dS_\xi = 0 \qquad (\mathbf{x} \text{ on } S_m), \qquad (3)$$

$$2\pi\phi^{(2)} + \iint_{S_m} \phi^{(2)} G_n^{(2)} dS_\xi - \iint_{S_m} G^{(2)} \phi_n^{(2)} dS_\xi = 4\pi\phi_I \qquad (\mathbf{x} \text{ on } S_m). \qquad (4)$$

The unknowns are $\phi^{(1)}$ on $S_b$, $\phi^{(2)}$ on $S_m$, and $\phi_n^{(2)}$ on $S_m$. The coupled integral equations (2-4) are discretized and solved using a modified version of the panel code WAMIT. The higher-order method is used, with the unknowns represented by B-splines. The surface $S_b$ is represented by explicit formulae and $S_m$ is a circular cylinder.

Before considering the objective of bed shapes which minimize the scattered energy, a simpler problem is considered to validate the procedure described above. A circular cylinder of unit radius is fixed on the bottom in an annular bed of constant depth $h_1$ with $h_2 = 1$, as shown in Figure 1(a). The exciting force is shown in Figure 1(b) for the cylinder alone and in (c) for the complete surface $S_b$, for several depths $h_1$. As $h_1$ is increased the force on the cylinder increases, whereas the total force on $S_b$ is decreased. For $h_1 \leq 1$ the results agree to several decimal places with computations using the conventional panel method without domain decomposition.

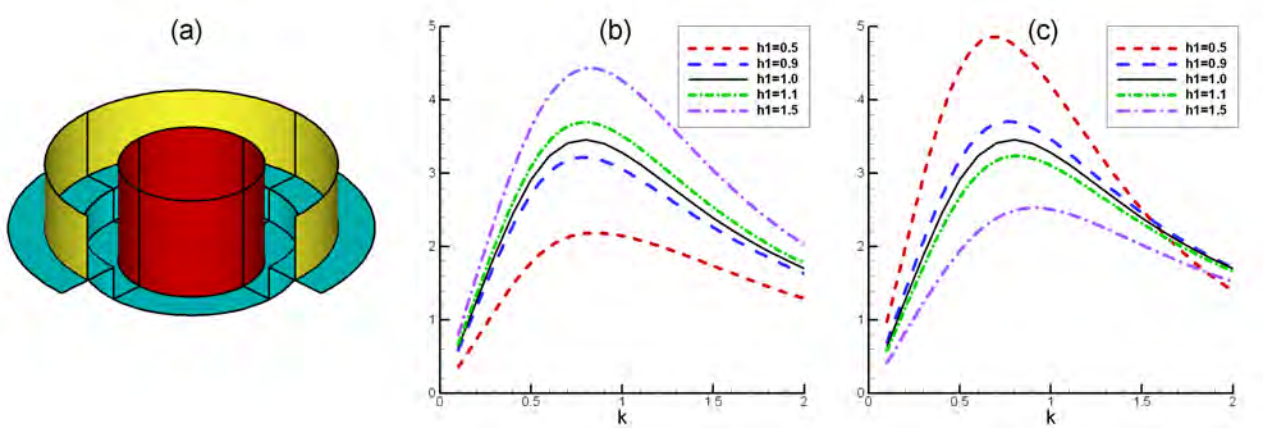


Figure 1: Perspective view (a) of the cylinder in a bed of depth $h_1$. (Part of one quadrant is omitted.) The depth outside the bed is 1.0, extending to infinity. The outer cylinder is the matching boundary, with radius $r = 2.0$ . The bed extends from the cylinder $r = 1.0$ to a cylindrical step at $r = 1.5$. The figure (b) shows the exciting force on the cylinder and (c) shows the combined force on the cylinder and bed, for different values of the depth $h_1$. The abscissa is the wavenumber $k$. The forces are normalized by the product of the fluid density, gravity, wave amplitude, and cylinder radius.

The scattered energy will be evaluated assuming incident waves of unit amplitude, frequency $\omega$ and wavenumber $k$, propagating at the angle $\theta = \beta$. The potential in the far field is

$$\phi^{(2)}(r,\theta,z) = \phi_I + \phi_S \simeq \frac{g}{\omega}\frac{\cosh\left(k(z+h_2)\right)}{\cosh(kh_2)}\left[\mathrm{e}^{-\mathrm{i}kr\cos(\theta-\beta)} + \frac{H(\theta)}{\sqrt{2\pi kr}}\,\mathrm{e}^{-\mathrm{i}kr-\pi\mathrm{i}/4}\right]. \tag{5}$$

Here $(r,\theta)$ are polar coordinates about the $z$-axis, $g$ is the gravitational acceleration, and the time-dependence is represented by the factor $\mathrm{e}^{\mathrm{i}\omega t}$. The Kochin function $H(\theta)$ can be evaluated from

$$H(\theta') = \frac{k}{2v_g}\iint_{S_m}\left(\phi_n^{(2)} - \phi^{(2)}\frac{\partial}{\partial n}\right)\frac{\cosh\left(k(z+h_2)\right)}{\cosh(kh_2)}\,\mathrm{e}^{\mathrm{i}kr\cos(\theta-\theta')}\,dS \tag{6}$$

where $v_g$ is the group velocity. The energy radiated by the scattered waves is proportional to

$$\mathcal{E} = \frac{1}{2\pi}\int_0^{2\pi}|H(\theta)|^2 d\theta = -2\mathrm{Im}\left\{H(\beta)\right\}. \tag{7}$$

This is referred to below as the scattered energy. The energy ratio is defined as the value of $\mathcal{E}$ for the bed, divided by the value for the cylinder in a constant depth $h_2$.

Figure 2(a) shows a perspective view of one of Porter's optimized beds. The cylinder radius is 0.5 and the bed occupies the annulus $0.5 < r < 5.0$. The depth outside the bed is 1.0. The depth of the bed is represented by a Fourier/Chebyshev expansion ([1], eq 25) with 8 coefficients (2 azimuthal and 4 radial), which are optimized using the mild-slope equation to achieve a minimum energy ratio equal to $1.6 \times 10^{-8}$ at $k = 1$. The results shown in Figure 2(b) are based on the present method with the matching boundary at $r = 5.0$. These results indicate that the energy ratio based on the complete linear theory is substantially larger.

Figures 3 shows four bed shapes with the same dimensions, which are optimized using the present method. The number of Fourier/Chebyshev coefficients and minimum value of $\mathcal{E}$ are shown for each bed. Figure 4(a) shows the scattered energy for each bed, and for the cylinder in constant depth $h_2$. The results for the cases (4,4) and (4,8) are similar, suggesting a modest degree of convergence. Figure 4(b) shows the mean drift force on the cylinder and 4(c) shows the total drift force on the cylinder and bed. The total drift force is positive, in accordance with momentum analysis, but the force on the cylinder is negative for the bed (2,4) near $k = 1$. For wavenumbers near 1.0 both drift forces are substantially reduced with the optimized beds, compared to the cylinder in constant depth $h_2$.

Since WAMIT is a single-precision code, it is likely that $\mathcal{E} = 0.00013$ is close to the practical limit that can be achieved with this program. This suggests, without a conclusive proof, that beds with no scattering in the far field do in fact exist, within the context of linear theory. Porter's bed shown in Figure 2 has a much smaller energy ratio based on the mild-slope approximation, but not according to the complete linear theory. Nevertheless its shape is similar to the beds shown in Figure 3, and the Fourier/Chebyshev expansion used by Porter is very useful as a basis for studying this problem.

## Acknowledgement

I am indebted to Richard Porter for suggesting this problem, advice on the optimization procedure, and sharing unpublished results for the bed shown in Figure 2.

## References

[1] Porter, R. 'Cloaking of a cylinder in waves,' IWWWFB26 (2011), Athens, Greece.

[2] Ferreira, M.D. & Newman, J.N. 'Diffraction effects and ship motions on an artificial seabed,' IWWWFB24 (2009), Zelenogorsk, Russia.

[3] Belibassakis K.A., 'A boundary element method for the hydrodynamic analysis of floating bodies in variable bathymetry regions,' Engineering Analysis with Boundary Elements, 32 (2008), 796-810.

[4] Pinkster, J.A. 'A multi-domain approach in 3-D diffraction calculations,' OMAE2011-49414 (2011), Rotterdam, Netherlands.

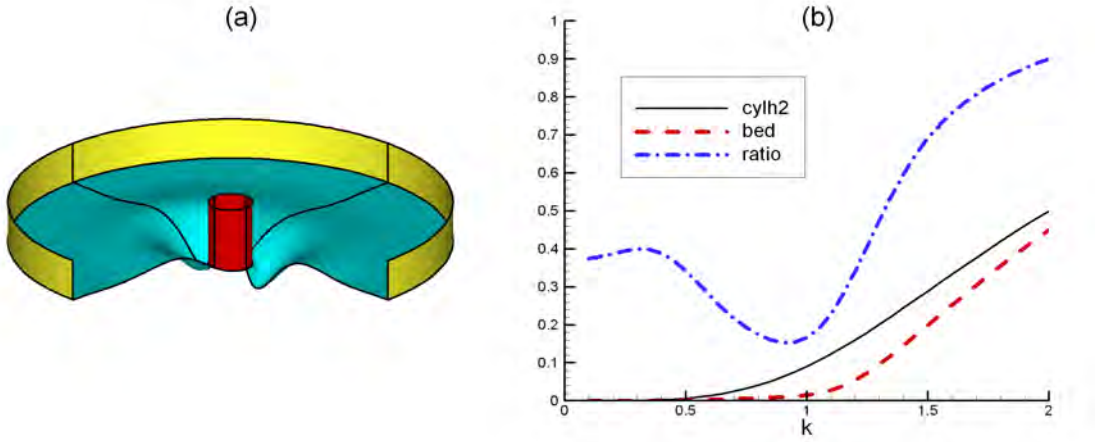


Figure 2: Perspective view of the Porter bed and cylinder (a) and the scattered energy (b). The outer cylinder shown in (a) and in Figure 3 is the matching boundary. The curve labeled 'cylh2' is the energy scattered by the cylinder in a fluid of constant depth $h_2$.

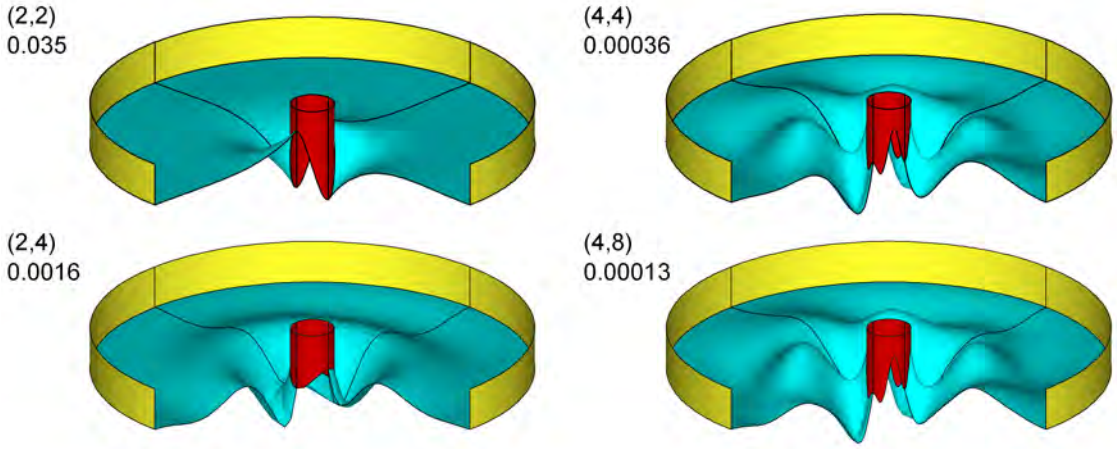


Figure 3: Perspective views of the cylinder with four beds which are optimized using the complete linear theory. The numbers of (Fourier,Chebyshev) modes are shown in parenthesis. The decimal number is the scattered energy at $k = 1$.

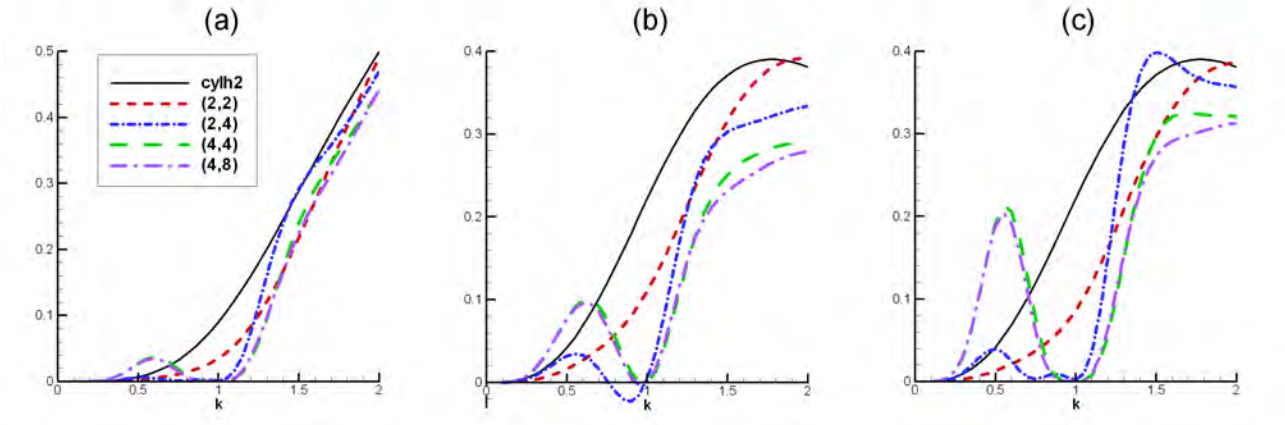


Figure 4: Scattered energy (a) and mean drift force (b-c) for the cylinder and optimized beds in Figure 3, compared with the cylinder in constant depth $h_2$. The drift force on the cylinder is shown in (b), and the combined force on the cylinder and bed in (c).